phys. stat. sol. (a) **56**, 597 (1979)

Subject classification: 14.4.1; 22.8.1

Fachrichtung 11.2 — Experimentalphysik der Universität Saarbrücken[1])

Dielectric Properties of Ferrielectric Ammonium Sulphate in the Microwave Region

By

G. LUTHER and H.-G. UNRUH

The ferroelectric dispersion of ammonium sulphate (AS) in the microwave region is studied. The dispersion is well described by a monodispersive Debye relaxation with a Curie-Weiss law $C_p/(T - T_0)$ for the dispersion step and a linear critical slowing down of the relaxation frequency f_ε. At the phase transition f_ε comes down to 23 GHz. The results are in agreement with the ferrielectric structure of AS and are discussed in terms of the coupled oscillator–relaxator model.

Es wird die ferroelektrische Dispersion von Ammoniumsulfat (AS) im Mikrowellenbereich untersucht. Die Dispersion läßt sich gut durch eine monodispersive Debye-Relaxation mit einem Curie-Weiss-Gesetz $C_p/(T - T_0)$ für die Dispersionsstufe und einem linearen kritischen Abfall der Relaxationsfrequenz f_ε beschreiben. Am Phasenübergang fällt f_ε auf 23 GHz ab. Die Ergebnisse sind in Übereinstimmung mit der ferrielektrischen Struktur von AS und werden mit dem gekoppelten Oszillator–Relaxator-Modell diskutiert.

1. Introduction

Ammonium sulphate (AS), $(NH_4)_2SO_4$, is a well-known ferroelectric substance, which undergoes at −50 °C a first-order phase transition. The space group changes from (orthorhombic) Pnam in the paraelectric phase to (orthorhombic) $Pna2_1$ in the ferroelectric phase. The crystal exhibits a unique temperature dependence of its spontaneous polarization, P_s, [1] which has been attributed to a ferrielectric structure [2] brought about by the presence of crystallographic nonequivalent and oppositely polarized sublattices. Great efforts have been made during the last few years for better understanding the nature of the phase transition. For a short review and references see [3]. The experimental facts support the assumption that at least two nonequivalent sublattices, which may be identified by the two different $(NH_4)^+$ sublattices, contribute to the spontaneous polarization. A soft mode could be detected neither in the infrared spectrum [4] down to 30 cm^{-1} nor in the Raman spectrum [5 to 7]. Several authors [8 to 11] have examined the microwave behaviour of AS, but because of restrictions in their frequency ranges or in the accuracy of their measurements no complete and consistent description of the ferroelectric dispersion is available. Therefore, we studied the dielectric properties of AS in the frequency range from 10^7 to 2×10^{10} Hz and report about the ferroelectric dispersion of the temperature-dependent dielectric constant. We can describe this dispersion by a simple Debye relaxation and receive Curie-Weiss laws for the dispersion step and for the relaxation time. The results are discussed in terms of the two nonequivalent sublattices model of Dvořak and Ishibashi [12] and in terms of the coupled oscillator–relaxator model introduced by Petzelt et al. [4] in the discussion of the dynamic behaviour of AS.

[1]) D-66 Saarbrücken, BRD.

2. Measuring Methods

The dielectric constant $\varepsilon^* = \varepsilon' - j\varepsilon''$ was measured at 1.6 kHz by a standard bridge (Wayne Kerr, B642). From 10^7 to 10^{10} Hz, we used the standard method for anisotropic crystals, where the sample is situated between the front side of the inner conductor of a coaxial line and a short piston. The samples had evaporated Au electrodes and were in good contact with a 0.1 mm thick Ag foil, which represents the front of the short piston and is pressed by a spring of a second piston (within the short piston) against the sample (Fig. 1). We used a 50 Ω line with an outer diameter of 14 mm. To the end of the line, however, the inner conductor was tapered to a diameter of 11 mm. The reflection coefficient of the sample was measured by the reflectometer method (with the Hewlett-Packard network analysers hp 8410 and hp 8407, for 0.1 to 12 GHz and 0.01 to 0.1 GHz, respectively). A careful two-port calibration with Ag, rutile and "air" replicas of the sample were made in temperature intervals of 25 K.

In the K-band (18 to 26 GHz) we used also a reflectometer method with the phase and amplitude receiver 1753 from Scientific Atlanta. The samples in the shape of rectangular plates were polished to exactly the dimensions of the standard waveguide and then glued with silver epoxy adhesive (EPO-TEK 410-E, Polytec) into a standard flange. The technique of polishing and mounting guaranteed a nearly perfect fit of the sample to the waveguide. The "sample-flange" was then connected to a movable disc with six waveguide ports, allowing to switch three samples and three offset shorts for calibration to the waveguide leading to the reflectometer. At each temperature and frequency several calibrations and sample measurements were done.

Over a broad frequency range we have to compare sensitive measurements on different samples. Therefore, the absolute values of the dielectric constant must be matched at one point because of unavoidable systematic errors in geometry, calibration, etc. Thus we have matched the values from the K-band to those of the coaxial measurements at room temperature, where no dispersion occurs and where losses are practically zero.

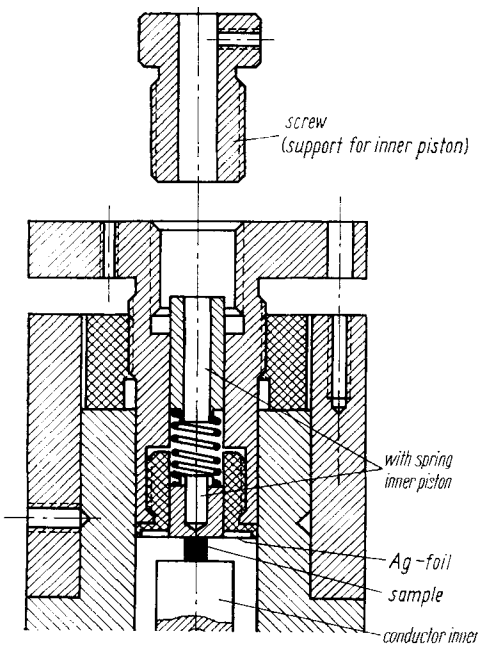

Fig. 1. The head of the sample holder

We report here about measurements on four samples from four different crystals. The crystals were grown from aqueous solution. The samples were prepared and shaped according to the demands of the different frequency ranges and measuring methods. The ferroelectric axis was parallel to the electric field. The geometrical data of the samples are the following:

sample	shape	geometry (mm)	used for frequency range
AS-2	disc	$\varnothing = 5.00$ $t = 0.967$	2 to 12 GHz
AS-3	disc	$\varnothing = 9.91$ $t = 0.506$	60 to 100 MHz
AS-9	plate	$t = 3.728$	K-band (18 to 26 GHz)
AS-13*)	plate	$t = 3.51$	K-band

*) The sample AS-13 has been in the ferroelectric state already before the measurements reported here.

3. Static Dielectric Properties

3.1 Above T_c

In the literature many measurements of static dielectric properties of AS were reported [13 to 17]. The data show considerable scatter. We assume a systematical error between these measurements, resulting from sample geometry and calibration errors, which can be accounted for by a multiplication factor. For comparing different measurements we fit all the data at 0 °C to our data from AS-3, which shows $\varepsilon'(0\ °C) = 9.63$. Then the static values of the dielectric constant at T_c of all measurements considered here are described by

$$\varepsilon_s(T_c + 0) = 12.72 \pm 0.2\,. \tag{1}$$

The remaining uncertainty does not come only from difficulties in getting the data from the published figures but also reflects a scatter in the true ε_s of different samples. Such we have found that two samples from different crystals which were measured simultaneously in one sample holder and with the same bridge nevertheless showed a difference in $\varepsilon_s(T_c + 0)$ of 0.13, although they were fitted to the same value at 0 °C. This difference is far above the resolution of the bridge.

Our static data, measured at high frequency but below the region of dispersion or corrected with the Debye formula (cf. Section 3), are

$$\left.\begin{aligned} \varepsilon_s(T_c + 0) &= 12.62 \quad \text{for AS-3}\,, \\ \varepsilon_s(T_c + 0) &= 12.79 \quad \text{for AS-2} \end{aligned}\right\} \tag{2}$$

and thus agree with (1). Below the ferroelectric dispersion in the 10^{10} Hz range, we could not find any other dispersion.

Usually the Curie-Weiss law

$$\varepsilon_s = \varepsilon_G + C_p/(T - T_0)\,, \tag{3}$$

with ε_G constant, is used to describe the paraelectric temperature dependence of the dielectric constant. A least-squares fit of our data to equation (3) showed, however, that the deviations though small are far from being random. Therefore, the formal correspondence between fitted and measured data may be doubted. In (3) a possible

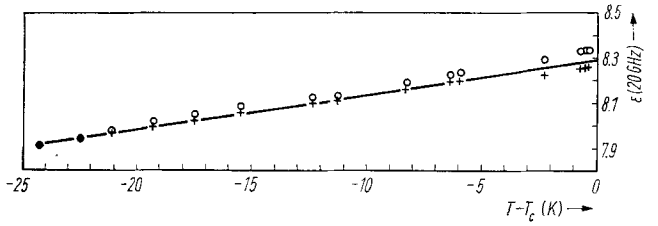

Fig. 2. Temperature dependence of domain clamped dielectric constant below T_c (measured at 20 GHz). + AS-9, ○ AS-13

temperature dependence of ε_G was neglected which may be significant because of the small temperature dependence of ε_s. Further, it is difficult to understand that ε_G is much greater than ε_∞ extrapolated from the dispersion measurements (cf. Section 3). A correct description on the basis of the Curie-Weiss law must therefore take into account the temperature dependence of $\varepsilon_\infty(T)$ and is discussed in Section 4.

3.2 Below T_c

At low frequencies the dielectric properties below T_c are characterized by large contributions from domain wall motions [13], which can be suppressed by application of dc bias [9]. Already in the 10^7 Hz range these domain wall contributions are totally clamped and we did not observe any frequency dependence of ε in our whole measuring range from 10^7 up to 2×10^{10} Hz. The values $\varepsilon(T_c - 0)$ of different samples (whose ε_s at room temperature were fitted by a calibration factor) were equal within a range of 0.15

$$\varepsilon'(T_c - 0) = 8.35 \pm 0.15\,. \tag{4}$$

The small scatter can be caused by small errors in the temperature corrections of the two port calibration and by different cracks of the samples, occurring always by going through the phase transition. The cracking is a serious problem, and we have only considered those samples, which afterwards gave again the original paraelectric values.

Also below T_c the temperature dependence cannot be overlooked (Fig. 2), the slope is

$$\frac{\Delta\varepsilon}{\Delta T} \approx 0.015\ \mathrm{K}^{-1}\,. \tag{5}$$

Recently, Yoshihara et al. [15] have reported that some degrees below T_c the static dielectric constant shows an additional anomaly. From our data we cannot deduce such an anomaly and suggest that the peak reported in [15] may be caused by the domain structure, which is responsible for a considerable part of the dielectric constant at low frequency.

4. Ferroelectric Dispersion

In the coaxial frequency range up to 10^{10} Hz we found strong dielectric losses, indicating the onset of the ferroelectric dispersion. For a fixed temperature, combining the data from the coaxial range with the 20 GHz data we got the Cole-Cole plot, shown in Fig. 3. As we must take the data from different samples, we must remember the uncertainty of ± 0.15 in the static values of the dielectric constant. In our measurements for example, there is a small difference in ε' between the actually measured

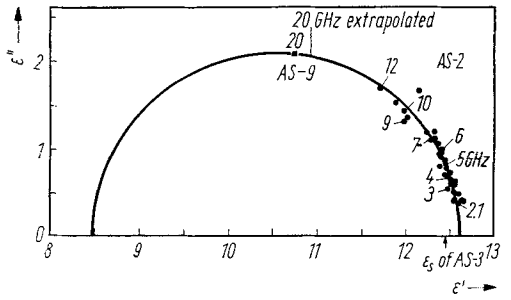

Fig. 3. Cole-Cole plot, 0.42 K above T_c, demonstrates the validity of monodispersive Debye behaviour. $T = 50.482$ °C

ε^*(20 GHz) (sample AS-9) and the 20 GHz point extrapolated from the 2 to 12 GHz measurement (sample AS-2), as demonstrated in Fig. 3. On the other hand, the static values measured with sample AS-3 show nearly the same small difference to the AS-2 data, suggesting that this combination may be a good choice. From Fig. 3 and from the fact that the frequency distribution of the AS-2 measurements corresponds well to the Debye formula

$$\varepsilon^*(\omega) = \varepsilon' - j\varepsilon'' = \varepsilon_\infty + \frac{\varepsilon_s - \varepsilon_\infty}{1 + j\nu/f_\varepsilon}, \tag{6}$$

we infer that the ferroeletric dispersion of AS is of the monodispersive Debye relaxation type.

We evaluated the parameters of equation (6) in two different ways:

Procedure A: From the static values $\varepsilon_s(T)$ of AS-3 and the accurate complex $\varepsilon^*(T)$ at 20 GHz of AS-9 we got $\varepsilon_\infty(T)$ (Fig. 4) and then $f_\varepsilon(T)$ (full circles in Fig. 5).

Procedure B: Here we calculated $f_\varepsilon(T)$ (open circles in Fig. 5) from the low frequency part of the dispersion measured with sample AS-2. We used $\varepsilon_\infty(T)$ from procedure A but corrected for the small differences between the static values of AS-3 and the corresponding values of the AS-2 measurements.

Naturally we could also calculate ε_∞ from the coaxial measurements alone, but then the accuracy would not be sufficient, because the frequency range covers only a small part of the dispersion region.

To demonstrate the sensitivity of the calculated value of ε_∞ to the difference $\varepsilon_s - \varepsilon'$(20 GHz) we solve equation (6) for

$$\varepsilon_\infty = \varepsilon' - \frac{\varepsilon''^2}{\varepsilon_s - \varepsilon'} \tag{7}$$

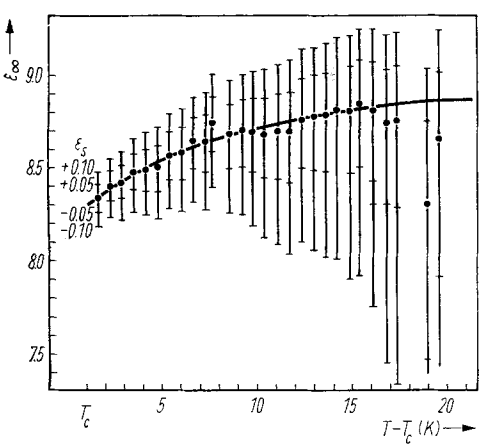

Fig. 4. $\varepsilon_\infty(T)$, the high frequency end of the ferroelectric dispersion (calculated from a measurement of ε_s in the frequency range between 60 and 110 MHz with sample AS-3 and from ε^* (20 GHz) with sample AS-9). The bars label a difference of $\pm$ 0.1 in ε_s ($\varepsilon_s + 0.1$ gives a higher value of ε_∞)

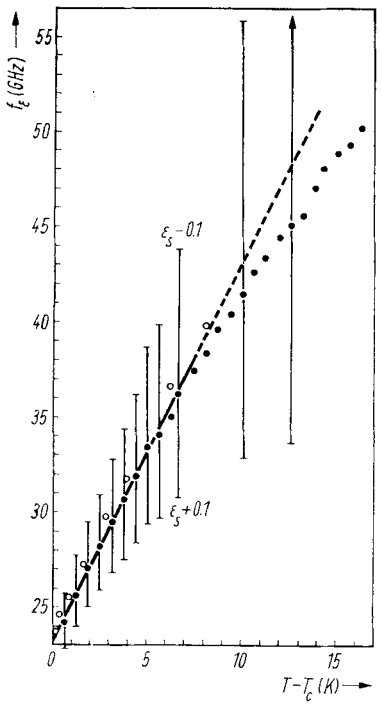

Fig. 5. Relaxation frequency $f_\varepsilon(T)$ of $(NH_4)_2SO_4$. ● f_ε calculated from static values of sample AS-3 and ε^* (20 GHz) of sample AS-9 (procedure A), ○ f_ε calculated from the measurements up to 12 GHz with sample AS-2, and $\varepsilon_\infty(T)$ as described in the text (procedure B). The deviations from the straight line, occurring for greater distance from T_c, may be irrelevant, because they may result from the combination of two different samples in a range where small errors result in extreme differences of the calculated quantity f_ε

and consider the residual scatter in the static dielectric constant, which is of the magnitude of 0.1 as mentioned above. This results in the bars given in Fig. 4 which give only a limit for a possible shift of the curve due to the use of different samples. But these great uncertainties correspond by no means to the statistical measurement errors, as is shown by the only slight deviations of the points around the curve. Thus we can reasonably trust the shape of $\varepsilon_\infty(T)$.

Taking carefully into account this uncertainty we can make the following statements:

1. The shape of $\varepsilon_\infty(T)$ in Fig. 4, especially the stronger decline of $\varepsilon_\infty(T)$ with T approaching T_c, is not very sensitive to the choice of $\varepsilon_s(T)$.

2. The slope of $\varepsilon_\infty(T)$ immediately above T_c is considerably greater than the slope of the clamped $\varepsilon(T)$ below T_c (Fig. 2).

3. We cannot be sure, that there is a continuous transition from $\varepsilon_\infty(T)$ in the paraelectric range to the clamped dielectric constant $\varepsilon(T)$ in the ferroelectric range, as is suggested by Fig. 2 and 4. Considering the scatter of $\varepsilon_s(T_c + 0)$ for different samples we estimate that a jump between $\varepsilon_\infty(T_c + 0)$ and $\varepsilon(T_c - 0)$ must be smaller than about 0.2. This sensitivity to the correct choice of ε_s could be only avoided by measuring at higher frequencies.

Fig. 5 shows the temperature dependence of the relaxation frequency f_ε, calculated according to both procedures described above. The line is drawn after the result from the 20 GHz measurement (procedure A). The continuous behaviour of the points ought not to tempt the interpretation that there are deviations from the linear dependence on $T - T_0$ at higher distances from T_c. In this range, the Debye parameters become extremely sensitive to the difference $\varepsilon_s - \varepsilon'(20\ \text{GHz})$, as is seen in Fig. 4 or equation (6). For example, at $T - T_c = 10$ K the static value ε_s should have to be smaller by 0.015, and at $T - T_c = 15$ K by 0.019 to bring the points on the straight line. Therefore, we have emphasized the points nearer to T_c and describe the temperature dependence of f_ε by

$$f_\varepsilon = \gamma(T - T_0') \qquad \text{with} \qquad \gamma = (2.0 \pm 0.15)\ \text{GHz/K} \tag{8}$$

and

$$T_c - T_0' = (11.6 \pm 1)\ \text{K}\,.$$

5. The Curie-Weiss Law for the Dielectric Susceptibility

Physically meaningful for the Curie-Weiss law is not the static dielectric constant ε_s but the dipolar susceptibility χ_D:

$$\chi_D = \varepsilon_s - \varepsilon_\infty = \frac{C_p}{T - T_0}. \tag{9}$$

If $\varepsilon_s(T)$ is much greater than ε_∞ — this is fulfilled for normal ferroelectrics —, the usually small T-dependence of ε_∞ can be neglected as a correction of higher order. In the case of AS, however, the static dielectric constant grows between 0 °C and the transition temperature $T_c = -50$ °C only from 9.6 to 12.7 and has the same magnitude as ε_∞. So the temperature dependence of $\varepsilon_\infty(T)$ becomes important for the correct description of the Curie-Weiss behaviour (9). With the ε_s data from sample AS-3 (measured between 60 and 100 MHz) and the $\varepsilon_\infty(T)$ data of Fig. 4 we have calculated by a least-squares fit the Curie-constant C_p and Curie-Weiss temperature T_0 according to (9). The differences between the measured points and the fit (Fig. 6), are in the whole range smaller than 0.008. If we add a constant ε_G to the right side of (9) and make a three-parameter least-squares fit for C_p, T_0, and ε_G for different numbers of points, this added quantity ε_G scatters around zero and amounts always to less than 0.05. We conclude that the Curie-Weiss law (9) for $\chi_D(T)$ is very well fulfilled and get the parameters

$$C_p = 39.0\ \text{K}\,, \qquad T_c - T_0 = 9.0\ \text{K}\,. \tag{10}$$

This analysis leads to a small difference between T_0 and T_0' in equations (10), (8), respectively.

6. Discussion

The description of the temperature dependence of ε_s by a Curie-Weiss law is not undisputed. So Onodera et al. [17] gave recently a phenomenological treatment of ferrielectrics in terms of two nonequilivalent sublattice polarizations, postulating a nonlinear equation for $\chi^{-1}(T)$. But their formula, although containing an additional fit parameter $T_1 + T_2$ compared to (3), does not give a convincing coincidence with their data. We think it is problematic to fit $\varepsilon_s(T)$ to complicated equations without an exact knowledge of the temperature dependence $\varepsilon_\infty(T)$, because ε_∞ has the same order of magnitude as ε_s. Moreover, Onodera et al. started from an expansion of the free energy only up to squares in the polarizations, which is not appropriate for the treatment of a first-order phase transition.

Starting from an higher-order expansion of a thermodynamic potential

$$\varphi = \tfrac{1}{2}\alpha_1 P_1^2 + \tfrac{1}{4}\beta_1 P_1^4 + \tfrac{1}{6}\delta P_1^6 + \tfrac{1}{2}\alpha_2 P_2^2 + \gamma_1 P_1 P_2 + \gamma_2 P_1^3 P_2 + \ldots \tag{11}$$

Dvořak and Ishibashi [12] studied the model with two nonequivalent sublattice polarizations (TNS model). Here P_i denotes a component of the i-th sublattice

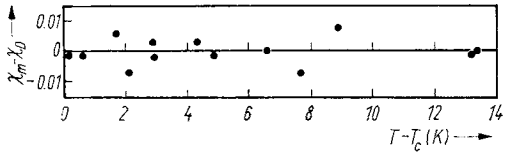

Fig. 6. The Curie-Weiss law for $\chi_D(T) = \varepsilon_s(T) - \varepsilon_\infty(T)$ is excellently fulfilled with the Curie constant $C_p = 39.0$ K and $T_c - T_0 = 9.0$ K. The figure shows the deviation of the measured points χ_m from the least-squares fit. Sample AS-3

polarization. Only the sublattice 1 is responsible for the phase transition

$$\alpha_1 = a_1(T - T_1)\,, \tag{12}$$

whereas α_2 is assumed to be temperature-independent in the paraelectric phase. The TNS model gives a phenomenological description of some outstanding properties of AS like the smallness of the Curie-Weiss constant (although AS is not an improper ferroelectric) and the change of the sign of the spontaneous polarization at low temperatures. The static dielectric susceptibility χ_p in the paraelectric phase is given by (equation (51) of [12])

$$\chi_p = \frac{1}{\alpha_2} + \frac{C}{T - T_c} \qquad \text{with} \qquad C = \frac{1}{a_1}\left(1 - \frac{\gamma_1}{\alpha_2}\right)^2. \tag{13}$$

The susceptibility χ_p in (13) contains contributions from both sublattice polarizations. In Section 4 we have shown that the microwave dispersion step $\varepsilon_s - \varepsilon_\infty$ is identical with the bare Curie-Weiss contribution (9). We conclude that the noncritical part of the polarization, P_2, which contributes the term $1/\alpha_2$, has a considerably higher dispersion frequency and is included in our quantity ε_∞

$$\varepsilon_\infty = \tilde{\varepsilon}_\infty + \frac{1}{\alpha_2}, \tag{14}$$

where $\tilde{\varepsilon}_\infty$ comprises the electronic and all remaining infrared parts of the dielectric response.

In [4] the dynamics of the phase transition of AS are discussed in terms of a coupled oscillator-relaxator model. The oscillator (translational polar mode at about 200 cm^{-1}) was studied by infrared measurements by Petzelt et al. [4]. The dispersion step was given as

$$\Delta\varepsilon_{ir} = 4.4 \tag{15}$$

and no softening was observed. In a phenomenological theory ([4] based on [18] and [19]) a linear coupling between a damped oscillator and a Debye relaxator was described by the potential energy

$$U = \tfrac{1}{2} m^* \omega_0^2 P^2 + \tfrac{1}{2} \chi_Q^{-1} Q^2 - \alpha PQ - EP\,. \tag{16}$$

The first term is the potential energy of the bare polarization oscillator P with an effective mass m^* and an eigenfrequency ω_0. The second term represents the contribution of a bare Q relaxator of a nonpolarizational nature and χ_Q is its static susceptibility. The third term involves a bilinear coupling constant α and in the last term the effect of an external field E is considered. Adding the kinetic energy $T = \frac{1}{2} m^* \dot{P}^2$ and the Rayleigh dissipation function

$$F = \tfrac{1}{2} m^* \Gamma \dot{P}^2 + \tfrac{1}{2} \tau \chi_Q^{-1} \dot{Q}^2 \tag{17}$$

(Γ is the damping constant of the P oscillator and τ the relaxation time of the Q relaxator), Petzelt et al. [4] get from the solution of the Lagrangian equations of motion a Debye equation for the dielectric susceptibility

$$\chi(\omega) = \frac{1}{m^* \omega_0^2} + \frac{\xi \chi(0)}{1 + j\omega\tau_D} \tag{18a}$$

with

$$\xi = \frac{\alpha^2 \chi_Q}{m^* \omega_0^2}, \tag{18b}$$

$$\tau_D = \frac{\tau}{1-\xi}, \tag{18c}$$

and

$$\chi(0) = \frac{1}{m^*\omega_0^2(1-\xi)}. \tag{18d}$$

Equation (18a) is restricted to the low frequency dispersion $\omega \approx 1/\tau$ and the fact is used that the frequency range of the resonance dispersion is well separated from the relaxation, $\omega_0 \gg 1/\tau$. Further we have used $\exp(+j\omega t)$ for the periodic time dependence. For getting the phase transition Petzelt et al. assumed that the bare Q relaxator softens approaching a temperature $\tilde{T}_0$:

$$\chi_Q = \frac{A}{T-\tilde{T}_0}, \tag{19}$$

leading to a Curie-Weiss dependence of the coupling strength ξ (from (19), (18b))

$$\xi = \frac{\alpha^2 A}{m^*\omega_0^2}(T-\tilde{T}_0)^{-1}. \tag{20}$$

The limit of stability is reached, when $\chi(0) \to \infty$, which means from (18d) $\xi \to 1$ and from (18c) $\tau_D \to \infty$. This occurs at the temperature

$$T_0 = \tilde{T}_0 + \frac{\alpha^2 A}{m^*\omega_0^2}. \tag{21}$$

So long we have sketched the theory of Petzelt et al. [4]. For the interpretation of our measured dielectric data, we must attend to the factor 4π coming from the cgs system in which the theoretical equations are written. Then we can identify

$$\chi_D(\omega) = \varepsilon^*(\omega) - \varepsilon_\infty = 4\pi\xi \frac{\chi(0)}{1+j\omega\tau_D} \tag{22}$$

with

$$\varepsilon_\infty = \frac{4\pi}{m^*\omega_0^2} + \tilde{\varepsilon}_\infty. \tag{23}$$

From (9), (22), (18d), (20), and using (21) we get

$$\chi_D(0) = \frac{C_p}{T-T_0} = 4\pi \frac{\alpha^2 A}{(m^*\omega_0^2)^2 (T-T_0)}, \tag{24}$$

hence

$$C_p = 4\pi \frac{\alpha^2 A}{(m^*\omega_0^2)^2}. \tag{25}$$

From [4] we can take the oscillator contribution (15)

$$4.4 = \frac{4\pi}{m^*\omega_0^2}. \tag{26}$$

The Curie-Weiss constant (10) gives with (25), (26)

$$\alpha^2 A = 25.3\ \mathrm{K}. \tag{27}$$

The Curie-Weiss temperature $\tilde{T}_0$ of the bare Q relaxator (19) is lower than T_0. From (21), (26), (27) we get

$$T_0 - \tilde{T}_0 = 8.9\ \mathrm{K}. \tag{28}$$

Equations (18c), (20), and (21) yield

$$\frac{\tau}{\tau_D} = (1 - \xi) = \frac{T - T_0}{T - \tilde{T}_0}. \tag{29}$$

Neglecting the difference between T_0' (cf. (8)) and T_0, which may be an artefact, we may insert in (29) the linear dependence (8) of $f_\varepsilon = 1/2\pi\tau_D'$ and get a linear dependence of the relaxation frequency $f_Q = 1/2\pi\tau$ of the bare Q relaxator:

$$f_Q = \gamma(T - \tilde{T}_0) \tag{30}$$

with the same slope $\gamma = 2.0$ GHz/K as for f_ε, but with the Curie-Weiss temperature $\tilde{T}_0$ of the Q relaxator (equation (19)).

Summarizing, our measurements of the Debye relaxation of $\varepsilon^*(\omega)$ in the microwave region are in accordance with the oscillator–relaxator model of Petzelt et al. [4] and furnish experimental values for some of the quantities involved in the theory. Through the linear coupling of the bare Q relaxator to the polar oscillator, the Q relaxator is activated in the dielectric spectrum. So we get for the "unpolar" Q relaxator the limit of stability $\tilde{T}_0$, the temperature dependence of the relaxation frequency and the product of dispersion strength and coupling factor squared.

Acknowledgements

For the dielectric bridge measurements we thank Dipl.-Phys. W. Eller, for technical assistance Mr. E. Meyer. This work has been supported by the Deutsche Forschungsgemeinschaft, Sonderforschungsbereich 130 "Ferroelektrika".

References

[1] H.-G. UNRUH, Solid State Commun. **8**, 1951 (1970).
[2] H.-G. UNRUH and U. RÜDIGER, J. Physique, **33**, C2-77 (1972).
[3] H.-G. UNRUH, J. KRÜGER, and E. SAILER, Ferroelectrics **20**, 3 (1978).
[4] J. PETZELT, I. GRIGAS, and I. MAYEROVA, Ferroelectrics **6**, 225 (1974).
[5] B. H. TORRIE, C. C. LIN, O. S. BINBREK, and A. ANDERSON, J. Phys. Chem. Solids **33**, 697 (1972).
[6] Z. IQBAL and C. W. CHRISTOE, Solid State Commun. **18**, 269 (1976).
[7] H.-G. UNRUH and O. AYERE, Ferroelectrics **12**, 181 (1976).
[8] L. COUTURE, S. LE MONTAGNER, J. LE BOT, and A. LE TRAON, C. R. Acad. Sci. (France) **242**, 1804 (1956).
[9] H. OSHIMA and E. NAKAMURA, J. Phys. Chem. Solids **27**, 481 (1966).
[10] A. BODI, R. BAICAN, and I. BARBUR, Acta phys. Polon. **A39**, 39 (1971).
[11] I. MESHKAUSKAS, A. ORLYUKAS, and I. GRIGAS, Soviet Phys. — Solid State **18**, 1811 (1976).
[12] V. DVOŘAK and Y. ISHIBASHI, J. Phys. Soc. Japan **41**, 548 (1976).
[13] H.-G. UNRUH, Phys. Letters (Netherlands) **17**, 8 (1965).
[14] A. SAWADA, S. OHYA, Y. ISHIBASHI, and Y. TAKAGI, J. Phys. Soc. Japan **38**, 1408 (1975).
[15] A. YOSHIHARA, T. FUJIMURA, and K. I. KAMIYOSHI, phys. stat. sol. (a) **34**, 369 (1976).
[16] K. OHI, J. OSAKA, and H. UNO, J. Phys. Soc. Japan **44**, 529 (1978).
[17] A. ONODERA, Y. SUGATA, and Y. SHIOZAKI, Solid State Commun. **27**, 243 (1978).
[18] A. SAWADA, Y. TAKAGI, and Y. ISHIBASHI, J. Phys. Soc. Japan **34**, 748 (1973).
[19] R. L. REESE, I. J. FRITZ, and H. Z. CUMMINS, Phys. Rev. B **7**, 4165 (1973).

(Received July 27, 1979)